frontiers in Astronomy and Space Sciences

METHODS
published: 06 March 2018
doi: 10.3389/fspas.2018.00005

On the Selection of High-z Quasars Using LOFAR Observations

Edwin Retana-Montenegro and Huub Röttgering*

Leiden Observatory, Leiden University, Leiden, Netherlands

We present a method to identify candidate quasars which combines optical/infrared color selection with radio detections from the Low Frequency ARray (LOFAR) at 150 MHz. We apply this method in a region of 9 square degrees located in the Boötes field, with a wealth of multi-wavelength data. Our LOFAR imaging in the central region reaches a rms noise of $\sim 50\,\mu$Jy with a resolution of $5''$. This is so deep that we also routinely detect, "radio-quiet" quasars. We use quasar spectroscopy from the literature to calculate the completeness and efficiency of our selection method. We conduct our analysis in two redshift intervals, $1 < z < 2$ and $2 < z < 3$. For objects at $1.0 < z < 2.0$, we identify 51% of the spectroscopic quasars, and 80% of our candidates are in the spectroscopic sample; while for objects at $2.0 < z < 3.0$ these numbers are 62 and 30%, respectively. We investigate the effect of the radio spectral index distribution on our selection of candidate quasars. For this purpose, we calculate the spectral index between 1,400 and 150 MHz, by combining our LOFAR-Boötes data with 1.4 GHz imaging of the Boötes field obtained with the Westerbork Synthesis Radio Telescope (WSRT), which has a rms noise of $\sigma \sim 28\,\mu$Jy with a resolution of $13'' \times 27''$. We find that 27% of the candidate quasars are detected at 1,400 MHz, and that these detected objects have a spectral index distribution with a median value of $\alpha = -0.73 \pm 0.07$. Using a flux density threshold of $S_{150MHz} = 1.50$ mJy, so that all the $\alpha > -1.0$ sources can be detected in the WSRT-Boötes map, we find that the spectral index distribution of the 21 quasars in the resulting sample is steeper than the general LOFAR-WSRT spectral index distribution with a median of $\alpha = -0.80 \pm 0.06$. As the upcoming LOFAR wide area surveys are much deeper than the traditional 1.4 GHz surveys like NVSS and FIRST, this indicates that LOFAR in combination with optical and infrared will be an excellent fishing ground to obtain large samples of quasars.

Keywords: quasars, active galactic nuclei, surveys, radio, extragalactic astronomy, photometry, spectroscopy

OPEN ACCESS

Edited by:
Paola Marziani, Osservatorio Astronomico di Padova (INAF), Italy

Reviewed by:
Andjelka Branislav Kovacevic, University of Belgrade, Serbia
Daniela Bettoni, Osservatorio Astronomico di Padova (INAF), Italy

****Correspondence:***
Edwin Retana-Montenegro
edwinretana@gmail.com;
eretana@strw.leidenuniv.nl

Specialty section:
This article was submitted to Milky Way and Galaxies, a section of the journal Frontiers in Astronomy and Space Sciences

Received: *31 July 2017*
Accepted: *31 January 2018*
Published: *06 March 2018*

Citation:
Retana-Montenegro E and Röttgering H (2018) On the Selection of High-z Quasars Using LOFAR Observations. Front. Astron. Space Sci. 5:5. doi: 10.3389/fspas.2018.00005

1. INTRODUCTION

In recent years, large spectroscopically confirmed quasar samples have become available (Croom et al., 2005; Schneider et al., 2010; Pâris et al., 2017). These quasar samples enabled statistical studies related to many topics, including the relation between the black holes (BHs) and their host galaxies (Kauffmann et al., 2003), BH growth across cosmic time (McLure and Dunlop, 2004), and the quasar environments (Ross et al., 2009; Retana-Montenegro and Röttgering, 2017). With the next generation of wide-field surveys such as Pan-STARRS (Kaiser et al., 2002, 2010), Dark Energy Survey (DES, Flaugher, 2005), and the future Large Synoptic Survey Telescope (LSST, Tyson, 2002),

such studies will be extended to the fainter quasars. A challenge in properly exploiting these surveys is the identification of quasars without spectroscopic observations.

Quasar surveys historically made use of the ultraviolet-excess (UVX) of the typical quasar spectrum (Sandage et al., 1965; Richards et al., 2002). This translates into a set of optical and near-infrared color cuts chosen to separate quasars from stars. However, for $z > 2$ quasars this selection begins to fail as one approaches the flux limit, due to photometric errors broadening the stellar locus, and quasar and stellar color distributions blending. The necessity to increase the efficiency of quasar surveys has led to the development of new selection techniques (MacLeod et al., 2010b; Yèche et al., 2010; Bovy et al., 2011; Kirkpatrick et al., 2011; Palanque-Delabrouille et al., 2011).

A way to separate high-z quasars from stars is to complement optical/infrared color cuts with a radio detection. By imposing a radio detection the stellar contamination is reduced significantly, as radio stars are very rare (Kimball et al., 2009). This approach has been successful in discovering quasars that otherwise might have been missed using typical color selection (McGreer et al., 2009; Bañados et al., 2015) such as red and dusty quasars (Glikman et al., 2004, 2012, 2013) and rare high-z quasars (Hook et al., 2002; McGreer et al., 2006; Zeimann et al., 2011).

LOFAR is a new European radio interferometer operating at frequencies 15–240 MHz (van Haarlem et al., 2013) and represents a milestone in terms of radio survey speed compared to existing telescopes. The LOFAR Surveys Key Science Project aims to carry out a tiered survey. At Tier-1 level, the LOFAR Two-metre Sky Survey (LoTSS, Shimwell et al. 2017) aims to cover the whole northern sky down to $\sim$100 μJy rms. Deeper tiers cover smaller areas in fields with extensive multi-wavelength data (see Röttgering et al., 2011) with the LOFAR Boötes field the first of these deep fields to reach Tier-2 depth (Retana-Montenegro and Röttgering, in preparation). These surveys will open the low-frequency electromagnetic spectrum for exploration, allowing unprecedented studies of the radio population across cosmic time and opening up new parameter space for searches for rare, unusual objects such as high-z radio quasars in a systematic way. Perhaps, one of the most tantalizing prospects are the 21 cm absorption line measurements using LOFAR along sight lines toward $z > 6$ radio quasars.

One of the possibilities to increase the efficiency in the selection of quasars is by combining optical/infrared quasar selection techniques with LOFAR radio data. With its high sensitivity, LOFAR should detect significantly more quasars in comparison with previous shallower radio surveys. Here we describe a method to select candidate quasars that combines optical/infrared color cuts with LOFAR radio detection.

2. METHODS

2.1. Method Overview

Candidate quasars are selected by complementing optical and near-infrared color cuts with a LOFAR detection. The selection method is summarized in the following points:

- Optical color cuts to select Lyα break objects, and to separate quasars from stars.
- Mid-infrared color cuts to identify the presence of AGN-heated dust, and to reduce the contamination from low-z star-forming galaxies.
- Imposing a LOFAR 5σ detection. This point guarantees that stellar contamination in the sample is negligible.
- Fitting the UV/optical to MIR SEDs of the candidate quasars sample to quasar templates. This allows us to select the best candidates and further eliminate nonquasar contaminants from the sample.

2.2. Optical Selection

2.2.1. Selection of Lyα Break Objects

The use of color selection to identify high-z objects was first proposed more than four decades ago (e.g., Meier, 1976a,b). Since then this approach has been applied successfully to select quasars up to $z \gtrsim 6$ (Fan et al., 2001; Willott et al., 2007). The multi-color selection for finding high-z quasars usually employs at least 3 bands: one containing the Lyα emission line, one blueward (the dropout band), and one redward. This translates into a set of colors that can be to used to locate the Lyα emission line.

2.2.2. Separating Quasars and Stars

Although, quasars are starlike in appearance their radiation mechanisms are different to those of stellar sources. Stars have approximately single-temperature black-body spectral energy distributions (SEDs) (Bisnovatyi-Kogan, 2001), whereas energetic processes sculpt the distinctive power-law SEDs of quasars (Davidson and Netzer, 1979). These differences in the SEDs imply that stars and quasars occupy different regions in colorspace (Fan, 1999). Thus, in principle, optical color cuts can be chosen to reject the majority of stars.

2.3. Mid-Infrared Selection

Although, stellar contamination is reduced using the previous points, some contamination will still remain from other objects like compact low-z star-forming galaxies. These star-forming systems present optical red colors mimicking those of quasars, which is likely caused by a strong Balmer break or dust-extincted continuum. Here, we impose the color cuts proposed by Lacy et al. (2007) and Donley et al. (2012) to the Spitzer/IRAC photometry to reduce contamination by star-forming galaxies in our quasar sample.

2.4. LOFAR Detection

With increasing redshift the Lyα emission moves through and out of the blueward optical bands, resulting in quasars having similar colors to stars. Thus, a selection method based only on color cuts becomes less efficient at higher redshifts, as quasars occupy regions that overlap with those occupied by a significant fraction of stellar sources. This is worst at $2.2 < z < 3.0$, where the optical colors of quasars become indistinguishable from those of stars (Fan, 1999; Richards et al., 2002, 2006). An alternative approach to improve the quasar selection in these regions is the incorporation of information provided by radio surveys (Richards et al., 2002; Ross et al., 2012). The number

of radio stars with faint optical fluxes is very small (Kimball et al., 2009), therefore, by imposing a radio detection the stellar contamination becomes negligible in our sample.

2.5. Visual Inspection

We carry out a visual inspection of the imaging data for each candidate quasar. This process allows us to reject contaminants such as low-z galaxies and objects with photometry contaminated by nearby bright objects. We accept candidate quasars with the following characteristics: stellar optical morphology; no bright neighbors in close proximity; and no blending issues. The radio counterparts in the LOFAR map are also examined to reject artifacts or misclassified radio-lobes.

2.6. Fitting the UV/Optical to MIR Spectral Energy Distributions of the Candidate Quasar Sample

Our selection method exploits a variety of quasar observational properties to identify them in our survey data. We apply color cuts that diminish the fraction of stars and star-forming galaxies in our samples. However, these procedures do not completely eliminate confusion with other types of objects. Therefore, as a final confirmation we fit quasar templates to their SEDs. We build SEDs spanning from the optical/UV to the MIR range to identify the candidate quasars. These SEDs are fitted to the quasar templates from the AGN template library presented by Salvato et al. (2009).

The SED fits are inspected visually. We look for the following unequivocal features in the SEDs of quasars: (i) the strong break by absorption at 1215Å (rest-frame), (ii) the Lyα emission line, and (iii) a rising or flat power-law in the IRAC bands. We examine each SED to assess the overall quality of the fit. In this way, we are able to eliminate nonquasar contaminants.

3. RESULTS

3.1. Selecting Candidate Quasars in the NDWFS-Boötes Field

In this section, we apply the selection method using the Boötes ancillary data and our Tier-2 LOFAR catalog following the points aforementioned.

3.1.1. Data

The 9.2 deg^2 region in Boötes covered by the NOAO Deep Wide Field Survey (NDWFS, Jannuzi and Dey 1999) has optical data available on the U_{spec}, B_w, R, I, and Z bands. All these filters are standard except the U_{spec} and B_w, which have better efficiency and a more uniform wavelength coverage than the U-Bessel and B-Johnson filters, respectively. Additionally, the Boötes field has multi-wavelength coverage spanning from X-rays to radio wavelengths. In the X-rays and UV regimes, it has been observed with the Chandra (Kenter et al., 2005) and GALEX (Martin et al., 2003) satellites. At infrared wavelengths, it was part of the NEWFIRM survey (J,H,K bands; Autry et al., 2003) and Spitzer Deep, Wide-Field Survey (SDWFS) with IRAC (Ashby et al., 2009). Finally, in the radio regime, the Boötes region has been observed at 1.4 GHz with the VLA (Becker et al., 1995) and WSRT (de Vries et al., 2002), and at 150MHz with GMRT (Williams et al., 2013) and LOFAR (Williams et al., 2016). In this work, we use the deep 150 MHz LOFAR imaging presented by Retana-Montenegro and Röttgering (in preparation), with a noise level of $1\sigma\sim50\,\mu$Jy with a spatial resolution of $5''$. We use AB magnitudes for all bands in our analysis. We assume the convention $S_\nu \propto \nu^{-\alpha}$, where ν is the frequency, α is the spectral index, and S_ν is the flux density as function of frequency.

3.1.2. Candidate Quasars Selection

To test our quasar selection method, we utilize spectroscopy data from the AGES survey (Kochanek et al., 2012). While the spectroscopic sample spans the range $0 < z < 5.8$, we limit our selection to the intervals $1.0 \leq z \leq 2.0$ and $2.0 \leq z \leq 3.0$. The reason for using these two redshift intervals is twofold. First, quasars in these intervals provide a good test for our selection method. Secondly, there are more spectroscopically confirmed quasars for the redshift intervals considered as compared to those available at $z > 3.0$.

Quasars at $1.0 \leq z \leq 2.0$ are frequently selected using the excess of ultra-violet flux in the u-band, which results in a bluer u-g color as compared to that of stars with the same visual color (e.g., the g-r color) (Richards et al., 2002). However, the NDWFS-Boötes bandpass system (U_{spec},B_w,R,I,Z) does not include a g filter found in other photometric systems such as the SDSS filter set (u,g,r,i,z) (Fukugita et al., 1996). But instead the non-standard U_{spec} (λ_c = 3590Å, FWHM=540Å) and B_w (λ_c = 4111Å, FWHM=1275Å) filters had been used. The main disadvantage of the U_{spec} and B_w filter combination is the significant wavelength overlap between the two filters. This implies that quasars at $1.0 \leq z \leq 2.0$ can not be efficiently selected using their $U_{spec}-B_w$ colors.

To optimally define the color cuts for candidate quasars at $1.0 < z < 2.0$, we generate a library of synthetic quasar spectra following the procedure described in detail by Retana-Montenegro et al. (in preparation). These spectra are convolved with the NDWFS-Boötes filter curves to calculate the colors for the selection of $1.0 < z < 2.0$ quasars. Based on the colors derived, we adopt the color cuts shown by magenta lines in the first panel of **Figure 1**. These color cuts are:

$$y \geq 1.89 \times x - 1.0 \ \wedge \ y \leq 1.89 \times x + 1.20$$
$$\wedge\, y \geq -1.37 \times x - 1.20 \ \wedge \ y \leq -1.37 \times x + 3.38,$$

where $y = B_w - R$ and $x = U_{spec} - Z$.

Based on the colors obtained from simulated quasar spectra, we derive the color cuts to select $2.0 \leq z \leq 3.0$ quasars. The color cuts adopted for the selection are the following:

$$-0.35 \leq R - I \leq 0.75 \quad \text{and} \quad -0.35 \leq B_w - R \leq 1.2.$$

To reduce contamination from low-z star-forming galaxies in our quasar samples we adopt in both redshift bins the color cuts proposed by Donley et al. (2012):

$$w \geq 0.08 \wedge z \geq 0.15,$$
$$z \geq 1.21 \times w - 0.27 \ \wedge \ z \leq 1.21 \times w + 0.27$$

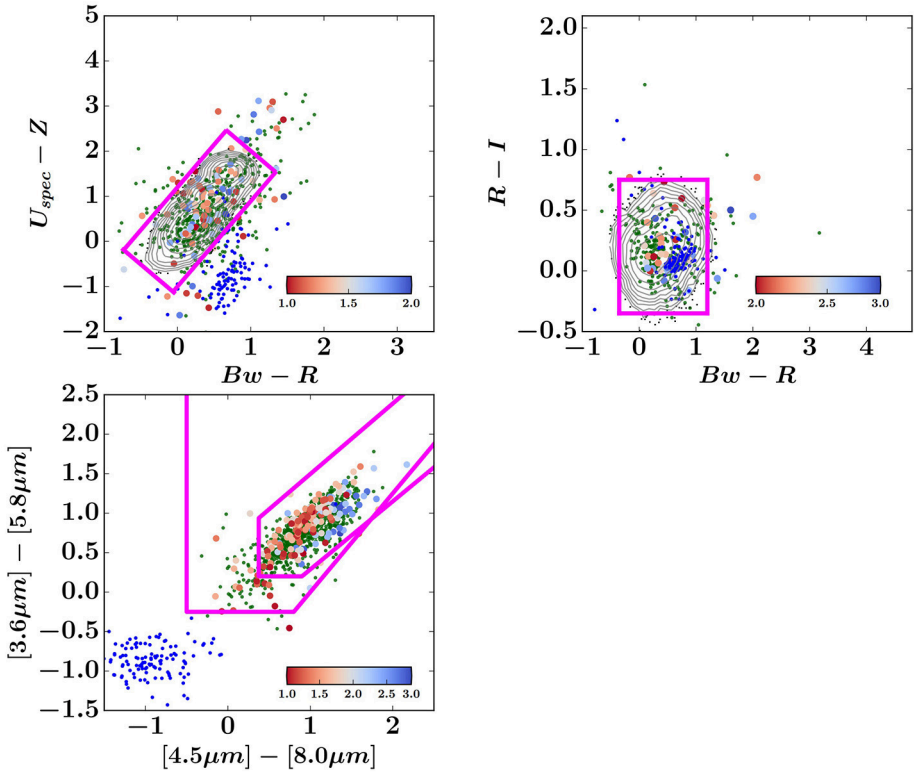

FIGURE 1 | Optical and mid-infrared colors for spectroscopic quasars in the Boötes field. The LOFAR detected quasars are plotted as redshift color-coded points according to the color bar at the lower right. The corresponding redshift bin is indicated by the colorbar legend. The dark green points represent spectroscopic quasars in the corresponding redshift that are undetected in our LOFAR observations, while the blue circles mark the location of stars. The solid magenta lines delimit the regions used to select the quasars in each color space. The gray contours denotes the density for 18,000 simulated quasars in the respective redshift bins.

and Lacy et al. (2007):

$$w > -0.1, z > -0.2,$$
$$z \leq 0.80 \times w + 0.5,$$

where $w = \log_{10}\left(\frac{S_{5.8\mu m}}{S_{3.6\mu m}}\right)$ and $z = \log_{10}\left(\frac{S_{8.0\mu m}}{S_{4.5\mu m}}\right)$.

Having defined the color cuts, the next task is to crossmatch the catalogs to find radio counterparts of the optical sources. We initially search for radio sources that lie within a radius of $2''$ from the optical source that fulfill our color cuts with a 5σ detection in our LOFAR catalog. For each one of these objects, we inspect its images in at least 4 bands. During this examination, we require that our candidate quasars are unresolved, not close to a bright neighbor and not blended. Additionally, we examine the morphology of the radio counterparts to prevent imaging artifacts or radio-lobes being incorrectly matched to optical sources. This examination of the radio maps ensures that only robust radio counterparts are matched to optical sources. Finally, we performed SED fitting to these sources with the photometric redshift code EAZY (Brammer et al., 2008). This allow us to assess the overall quality of the quasars photometry and to filter out contaminants from our sample. **Figure 2** shows two candidate quasars SEDs from our sample.

An important aspect to consider is the accuracy of the photometric redshifts. An inaccurate photometric redshift may cause the rejection of a quasar candidate. In **Figure 3**, we compare the EAZY z_{photo} and z_{spec} in the range $1.0 < z < 3.0$ for Boötes spectroscopic quasars with a signal-to-noise greater than 5σ. The objects that are catastrophic outliers (i.e., objects with a difference between the photometric and spectroscopic redshift larger than the 3σ uncertainty for the photometric redshift) based on the one-to-one relation are found using an iterative 3σ-clipped standard deviation. The fraction of catastrophic outliers is around 3.1%. After catastrophic outliers are eliminated, we compute the standard dispersion $\delta z = (z_{photo} - z_{spec})/(1 + z_{spec})$ (Ilbert et al., 2006), and the normalized median absolute deviation (NMAD), defined as $\mathrm{NMAD}(\delta z) = 1.48 \times \mathrm{Median}(\delta z)$ (Hoaglin et al., 1983). We find $\delta z = 0.15$ and NMAD $= 0.12$. For comparison, Salvato et al. (2011) obtained more accurate photometric redshifts for COSMOS quasars with NMAD $= 0.015$ using 30 bands, while Assef et al. (2010) found $\delta z = 0.18$ for point-source AGNs in Boötes. Therefore, we conclude that fraction of candidates quasars rejected with inaccurate z_{photo} is small in comparison with the total number of candidates in the final sample.

The optical and MIR colors of the spectroscopic quasars detected by LOFAR in the Boötes field are shown in

Figure 1. The colors of the spectroscopic quasars are generally consistent with the proposed color cuts. **Figure 4** shows the colors for the 154 candidate quasars selected using our method.

3.1.3. Performance of the Selection Method

In order to assess the performance of our selection method, we calculate the completeness and efficiency for our samples.

We define the completeness C as the number of spectroscopic quasars selected as candidates compared to the *total* number of spectroscopic quasars (Hatziminaoglou et al., 2000; MacLeod et al., 2010a):

$$C = \frac{\text{no. of selected spectroscopic quasars}}{\text{total no. of spectroscopic quasars}} \times 100.$$

Similarly, the efficiency E, i.e., the number of spectroscopic quasars selected as candidates compared to the number of objects selected as candidate quasars, is defined as:

$$E = \frac{\text{no. of selected spectroscopic quasars}}{\text{total no. of candidate quasars}} \times 100.$$

At $1.0 < z < 2.0$, our selection method identifies 59 of the 116 radio quasars with spectroscopic confirmation, resulting in a completeness of 51%. In the range $2.0 < z < 3.0$, 25 of 40 quasars pass our selection, which results in a completeness of 62%. For the entire redshift interval considered, we obtain a completeness of 54%.

With our method, we find 74 quasars candidates at $1.0 < z < 2.0$, which corresponds to an efficiency of 80%. In the range $2.0 < z < 3.0$, 84 candidate quasars are identified, which gives $E = 30\%$. For the full range, we find an efficiency equal to $E = 53\%$.

3.1.4. Effect of the Radio Spectral Index Distribution on the Candidate Quasar Selection

In this section, we investigate the effect of the radio spectral index distribution on our selection of candidate quasars. We therefore combine our LOFAR data with the deep 1.4 GHz radio survey of the Boötes field obtained using the Westerbork Synthesis Radio

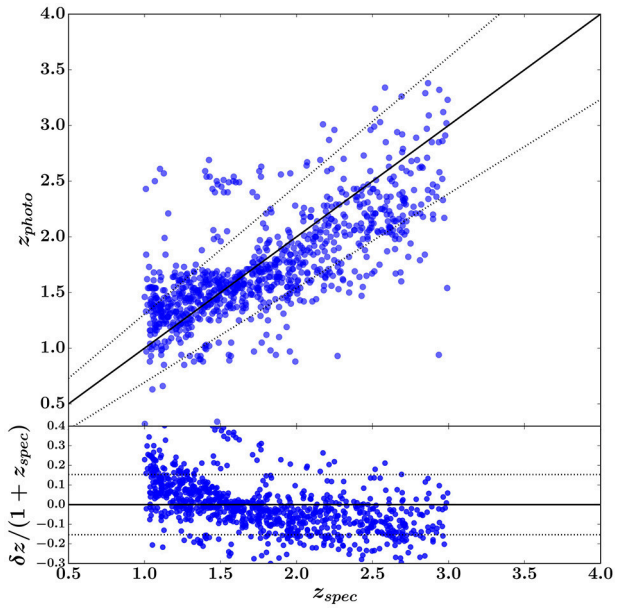

FIGURE 3 | (Top panel) Comparison between photometric and spectroscopic redshifts for 929 quasars in the Boötes field at $1.0 < z < 3.0$. The solid line represents the one-to-one $z_{phot} = z_{spec}$ relation, and the dotted lines correspond to $z_{phot} = z_{spec} \pm \sigma \times (1 + z_{spec})$. **(Bottom panel)** Standard dispersion between photometric and spectroscopic redshifts as function of the spectroscopic redshift. The solid and dotted lines are the same as in the top panel.

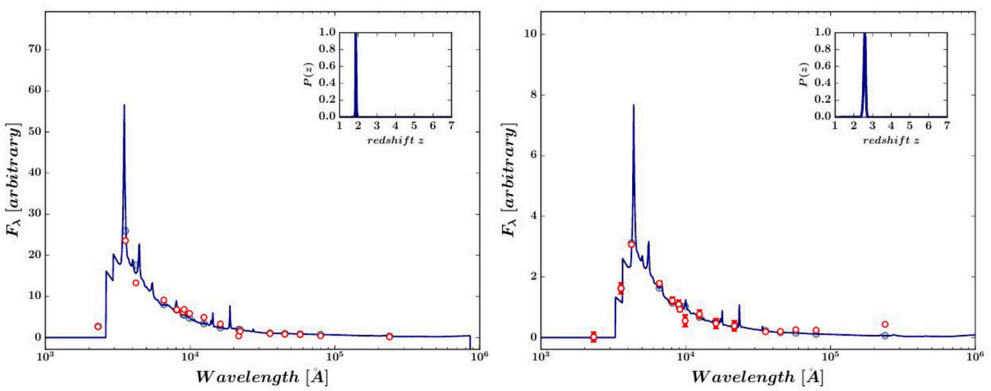

FIGURE 2 | Typical examples of the spectral energy distribution for two candidate quasars identified using our selection method. In each case the best-fit quasar template (as derived from the EAZY calculation) is also plotted. Red circles are the photometric points and the blue circles indicate the predicted photometry by the best-fit template. The phometric redhifts for objects are 1.87 and 2.57, respectively. The probability density distributions (PDFs) for each object are shown in the small inset. These PDFs strongly suggest that these objects are located at high-z. The Lyα line in the two candidate quasars is clearly identified as an abrupt break in the quasar SED between the NUV-GALEX band and U_{spec} and B_W filters, respectively.

Telescope (WSRT) telescope (de Vries et al., 2002). The WSRT-Boötes observations reach a rms noise of $1\sigma \sim 28\,\mu$Jy, with an angular resolution of $13'' \times 27''$. To compare the LOFAR and WSRT maps, we must take into account that there are incompleteness effects due to the different noise levels between the two observations. Therefore, we compare the LOFAR and WSRT observations using a flux density threshold of $S_{150MHz} = 1.5$mJy. For a spectral index of -0.7 (Smolčić et al., 2017), this threshold is approximately equivalent to a noise level of 11σ in the WSRT-Boötes map, and ensures all the $\alpha > -1.0$ sources with a signal-to-noise $> 5\sigma$ will be detected in the WSRT-Boötes map. The spectral index distribution for the 1998 sources in the LOFAR-WSRT sample has a median of $\alpha = -0.65 \pm 0.016$.

Using these cuts, in the overlapping area between the LOFAR and WSRT maps, we find that 42 of 154 candidate quasars are detected at 1,400 MHz. The detected objects have a spectral index distribution with a median value of $\alpha = -0.73 \pm 0.07$ (see **Figure 5**). Using the flux density threshold of $S_{150MHz} \geq 1.50$ mJy, we find that the spectral index distribution of the 21 candidate quasars in this sample is steeper than the general LOFAR-WSRT spectral index distribution with a median of $\alpha = -0.80 \pm 0.06$. The 21 candidate quasars detected at $1,400MHz$ with $S_{150MHz} < 1.5$ mJy are characterized by a steeper spectral index distribution compared to the LOFAR full sample with a median value of $\alpha = -0.71 \pm 0.05$. For the remaining 112 candidates undetected by WSRT, we derive an upper limit for their spectral indices assuming a 5σ WSRT detection ($S_{1.4GHz} = 0.140$ mJy). The median upper limit of the distribution of spectral indexes for these objects is $\alpha_{upp} < -0.75$. In the WSRT footprint, there are 70 of 139 spectroscopic quasars detected by WSRT. These detected quasars have a steeper distribution of spectral indices compared to the LOFAR-WSRT full sample with a median of $\alpha = -0.70 \pm 0.06$.

4. LIMITATIONS

The application of the selection method described in this work is dependent on the availability of LOFAR imaging and ancillary data. Fortunately, the dedicated LOFAR Tier-2 program selects extra-galactic fields with extensive multi-wavelength data to maximize the scientific exploitation of the LOFAR imaging. The ongoing LoTSS survey aims to map the observable northern sky, which has been observed previously in the optical (SDSS, York et al., 2000 and Pan-STARRS, Kaiser et al., 2002, 2010) and MIR (WISE, Wright et al., 2010) wavelengths. These LOFAR datasets will allow us to extend the identification of candidate quasars to a larger survey volume and to smaller regions with extensive multi-wavelength data.

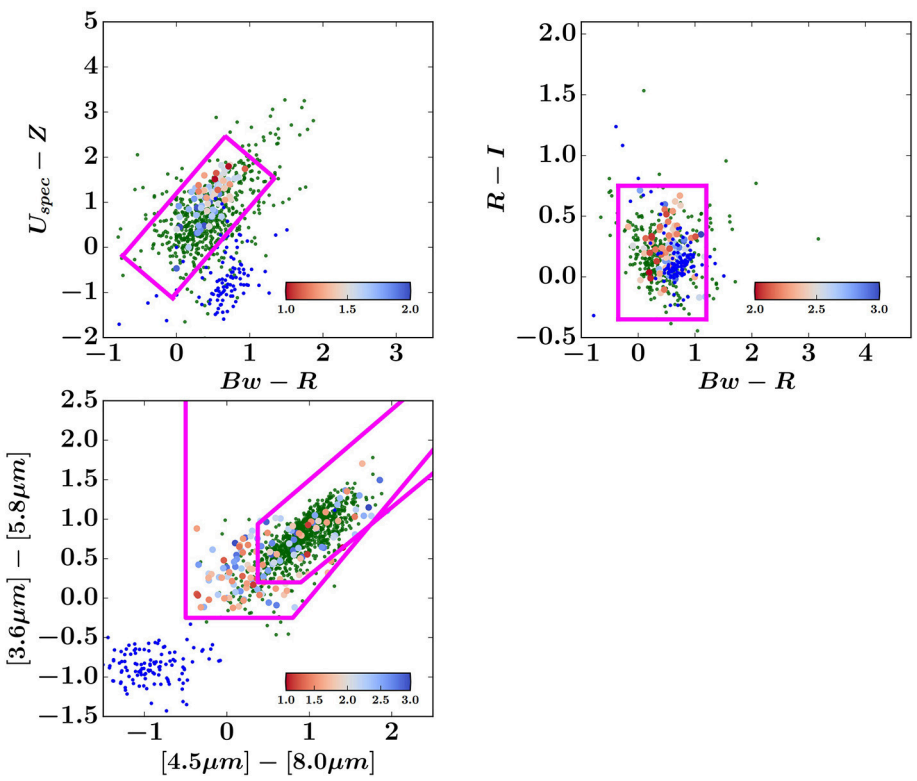

FIGURE 4 | Optical and mid-infrared colors for the candidate quasars identified within our selection regions (solid magenta lines). The color-scale indicates the photometric redshift for the candidate quasars. The dark green points represent all the spectroscopic quasars (both undetected and detected by LOFAR) in the Boötes region, while the blue circles mark the location of stars. The corresponding redshift bin is indicated by the colorbar legend.

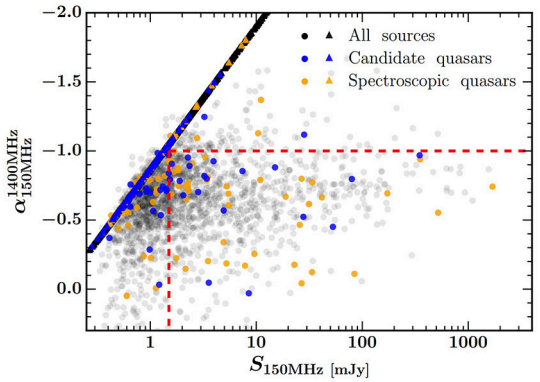

FIGURE 5 | The spectral index between 1,400 and 150 MHz for sources in the Boötes field as a function of the 150 MHz flux density. The candidate quasars, spectroscopic quasars, and all the sources in LOFAR catalog are shown by blue, orange and black markers, respectively. The circles denote 5σ detections in the LOFAR and WSRT catalogs, while the triangles indicate upper limits on the spectral indexes assuming a 5σ WSRT detection ($S_{1.4GHz} = 0.140$ mJy) for these objects. The red dashed lines indicate the region with $S_{150MHz} > 1.5$ mJy and $\alpha > -1.0$.

5. SUMMARY

We have examined the identification of high-z candidate quasars with LOFAR observations as an additional tool. The motivation for our method was to compile large samples of candidate quasars and to improve the efficiency of spectroscopic programs targeting these objects. Our selection method adopts color cuts between near-infrared and optical wavelengths to obtain a list of candidate quasars, while minimizing the contamination by stars and star-forming galaxies. Second, a LOFAR detection is required to further reduce the stellar contamination in our sample. We also carried out a visual inspection of candidate quasar SEDs to discard nonquasar contaminants. We used the LOFAR Tier-2 Boötes observations as an example of the application of our method and examined its completeness and efficiency in various redshift intervals. We also investigated the effect of the radio spectral index distribution on our selection of candidate quasars. For this purpose, we calculated the spectral index between 1,400 and 150 MHz, by combining our LOFAR data with WSRT-Boötes imaging. We found that the candidate quasars have a steep distribution of spectral indexes with a median value of $\alpha = -0.73 \pm 0.07$.

In conclusion, this work demonstrates that our selection method combining radio detections from LOFAR with optical/infrared color cuts will provide an excellent approach for obtaining large samples of quasars.

AUTHOR CONTRIBUTIONS

ER-M reduced the LOFAR Boötes data and carried out the source selection, as well as writing most of the text. HR contributed with ideas to the text writing.

FUNDING

ER-M acknowledges financial support from NWO Top project, No. 614.001.006. HR acknowledges support from the ERC Advanced Investigator program NewClusters 321271.

REFERENCES

Ashby, N. P., Stern, D., Brodwin, M., Griffith, R., Eisenhardt, P., Kozłowski, S., et al. (2009). The spitzer deep, wide-field survey. *Astrophys. J.* 701:428. doi: 10.1088/0004-637X/701/1/428

Assef, R. J., Kochanek, C. S., Brodwin, M., Cool, R., Forman, W., Gonzalez, A. H., et al. (2010). Low-resolution spectral templates for active galactic nuclei and galaxies from 0.03 to 30 μm. *Astrophys. J.* 713, 970–985. doi: 10.1088/0004-637X/713/2/970

Autry, R. G., Probst, R. G., Starr, B. M., Abdel-Gawad, K. M., Blakley, R. D., Daly, P. N., et al. (2003). Instrument design and performance for optical/infrared ground-based telescopes. *SPIE* 4841, 525–539. doi: 10.1117/12.460419

Bañados, E., Venemans, B. P., Morganson, E., Hodge, J., Decarli, R., Walter, F., et al. (2015). Constraining the radio-loud fraction of quasars at z ˜ 5.5. *Astrophys. J.* 804:118. doi: 10.1088/0004-637X/804/2/118

Becker, R. H., White, R. L., and Helfand, D. J. (1995). The FIRST survey: faint images of the radio sky at twenty centimeters. *Astrophys. J.* 450:559. doi: 10.1086/176166

Bisnovatyi-Kogan, G. S. (2001). *Stellar Physics. Vol.1: Fundamental Concepts and Stellar Equilibrium*. Astronomy and Astrophysics Library. (Trans.) A. Y. Blinov and M. Romanova. Berlin: Springer.

Bovy, J., Hennawi, J. F., Hogg, D. W., Myers, A. D., Kirkpatrick, J. A., Schlegel, D. F., et al. (2011). Think outside the color box: probabilistic target selection and the SDSS-XDQSO quasar targeting catalog. *Astrophys. J.* 729:141. doi: 10.1088/0004-637X/729/2/141

Brammer, G. B., van Dokkum, P. G., and Coppi, P. (2008). EAZY: a fast, public photometric redshift code. *Astrophys. J.* 686, 1503–1513. doi: 10.1086/591786

Croom, S. M., Boyle, B. J., Shanks, T., Smith, R. J., Miller, L., Outram, P. J., et al. (2005). Probing the radio loud/quiet AGN dichotomy with quasar clustering. *Month. Notices RAS* 356, 415–438. doi: 10.1111/j.1365-2966.2004.08379.x

Davidson, K., and Netzer, H. (1979). The emission lines of quasars and similar objects. *RevModPhys* 51, 715–766. doi: 10.1103/RevModPhys.51.715

de Vries, W. H., Morganti, R., Röttgering, H. J. A., Vermeulen, R., van Breugel, W., Rengelink, R., et al. (2002). Deep westerbork 1.4 GHz imaging of the bootes field *Astron. J.* 123, 1784–1800. doi: 10.1086/338906

Donley, J. L., Koekemoer, A. M., Brusa, M., Capak, P., Cardamone, C. N., Civano, F., et al. (2012). A new infrared color criterion for the selection of 0>z>7 AGNs: application to deep fields and implications for JWST surveys. *Astrophys. J.* 748:142.

Fan, X. (1999). Simulation of stellar objects in SDSS color space. *Astron. J.* 117, 2528–2551. doi: 10.1086/300848

Fan, X., Narayanan, V. K., Lupton, R. H., Strauss, M. A., Knapp, G. R., Becker, R. H., et al. (2001). A survey of z>5.8 quasars in the sloan digital sky survey. I. Discovery of three new quasars and the spatial density of luminous quasars at z=6. *Astrophys. J.* 122, 2833–2849. doi: 10.1086/324111

Flaugher, B. (2005). The dark energy survey. *IJMPA* 20, 3121–3123. doi: 10.1142/S0217751X05025917

Fukugita, M., Ichikawa, T., Gunn, J. E., Doi, M., Shimasaku, K., and Schneider, D. P. (1996). The sloan digital sky survey photometric system. *Astron. J.* 111:1748. doi: 10.1086/117915

Glikman, E., Gregg, M. D., Lacy, M., Helfand, D. J., Becker, R. H., and White, R. L. (2004). FIRST-2Mass sources below the APM detection threshold: a population of highly reddened quasars. *Astrophys. J.* 607, 60–75. doi: 10.1086/383305

Glikman, E., Urrutia, T., Lacy, M., Djorgovski, S. G., Mahabal, A., Myers, A. D., et al. (2012). FIRST-2MASS red quasars: transitional objects emerging from the dust. *Astrophys. J.* 757:51. doi: 10.1088/0004-637X/757/1/51

Glikman, E., Urrutia, T., Lacy, M., Djorgovski, S. G., Urry, M., Croom, S., et al. (2013). Dust reddened quasars in FIRST and UKIDSS: beyond the tip of the iceberg. *Astrophys. J.* 778:127. doi: 10.1088/0004-637X/778/2/127

Hatziminaoglou, E., Mathez, G., and Pelló, R. (2000). Quasar candidate multicolor selection technique: a different approach. *Astron. Astrophys.* 359, 9–17.

Hoaglin, D. C., Mosteller, F., and Tukey, J. W. (edS.). (1983). "Understanding robust and exploratory data analysis," in *Wiley Series in Probability and Mathematical Statistics*, (New York, NY: Wiley).

Hook, I. M., McMahon, R. G., Shaver, P. A., and Snellen, I. A. G. (2002). Discovery of radio-loud quasars with redshifts above 4 from the PMN sample. *Astron. Astrophys.* 391, 509–517. doi: 10.1051/0004-6361:20020869

Ilbert, O., Arnouts, S., McCracken, H. J., Bolzonella, M., Bertin, E., Le Fèvre, O., et al. (2006). Accurate photometric redshifts for the CFHT legacy survey calibrated using the VIMOS VLT deep survey. *Astron. Astrophys.* 457, 841–856. doi: 10.1051/0004-6361:20065138

Jannuzi, B. T., and Dey, A. (1999). Photometric redshifts and the detection of high redshift galaxies. *ASPCS* 191:111.

Kaiser, N., Aussel, H., Burke, B. E., Boesgaard, H., Chambers, K., Chun, M. R., et al. (2002). Pan-STARRS: a large synoptic survey telescope array. *Proc. SPIE* 4836, 154–164. doi: 10.1117/12.457365

Kaiser, N., Burgett, W., Chambers, K., Denneau, L., Heasley, J., Jedicke, R., et al. (2010). The pan-STARRS wide-field optical/NIR imaging survey. *Proc. SPIE* 7733. doi: 10.1117/12.859188

Kauffmann, G., Heckman, T. M., Tremonti, C., Brinchmann, J., Charlot, S., White, S. D. M., et al. (2003). The host galaxies of active galactic nuclei. *Month. Notices RAS* 346:1390. doi: 10.1111/j.1365-2966.2003.07154.x

Kenter, A., Murray, S. S., Forman, W. R., Jones, C., Green, P., Kochanek, C. S., et al. (2005). An X-ray survey of the NDWFS bootes field. II. The X-ray source catalog. *Astrophys. J. Suppl.* 161:9. doi: 10.1086/444379

Kimball, A. E., Knapp, G. R., Ivezić, Ž., West, A. A., Bochanski, J. J., Plotkin, R. M., et al. (2009). A sample of candidate radio stars in first and SDSS. *Astrophys. J.* 701, 535–546. doi: 10.1088/0004-637X/701/1/535

Kirkpatrick, J., Schlegel, D. J., Ross, N. P., Myers, A. D., Hennawi, J. F., Sheldon, E. S., et al. (2011). A simple likelihood method for quasar target selection. *Astrophys. J.* 743:2. doi: 10.1088/0004-637X/743/2/125

Kochanek, C. S., Eisenstein, D. J., Cool, R. J., Caldwell, N., Assef, R. J., Jannuzi, B. T., et al. (2012). AGES: the AGN and galaxy evolution survey. *Astrophys. J. Suppl.* 200:8. doi: 10.1088/0067-0049/200/1/8

Lacy, M., Petric, A. O., Sajina, A., Canalizo, G., Storrie-Lombardi, L. J., Armus, L., et al. (2007) Optical spectroscopy and X-ray detections of a sample of quasars and active galactic nuclei selected in the mid-infrared from two spitzer space telescope wide-area surveys. *Astron. J.* 133, 186–206. doi: 10.1086/509617

MacLeod, C. L., Brooks, K., Ivezic, Z., Kochanek, C. S., Gibson, R., Meisner, A., et al. (2010a). Quasar selection based on photometric variability. *Astrophys. J.* 728:16. doi: 10.1088/0004-637X/728/1/26

MacLeod, C. L., Ivezić, Ž., Kochanek, C. S., Kozłowski, S., Kelly, B., Bullock, E., et al. (2010b). Modeling the time variability of SDSS stripe 82 quasars as a damped random walk. *Astrophys. J.* 721:1014. doi: 10.1088/0004-637X/721/2/1014

Martin, C., Barlow, T., Barnhart, W., Bianchi, L., Blakkolb, B. K., Bruno, D., et al. (2003). The galaxy evolution explorer. *Proc. SPIE* 4854, 336–350. doi: 10.1117/12.460034

McGreer, I. D., Becker, R. H., Helfand, D. J., and White, R. L. (2006). Discovery of a z = 6.1 radio-loud quasar in the NOAO deep wide field survey. *Astrophys. J.* 652, 157–162. doi: 10.1086/507767

McGreer, I. D., Helfand, D. J., and White, R. L. (2009). Radio-selected quasars in the sloan digital sky survey. *Astron. J.* 138, 1925–1937. doi: 10.1088/0004-6256/138/6/1925

McLure, M. J., and Dunlop, J. S. (2004). The cosmological evolution of quasar black hole masses. *Month. Notices RAS* 352:1390. doi: 10.1111/j.1365-2966.2004.08034.x

Meier, D. L. (1976a). Have primeval galaxies been detected. *Astrophys. J.* 203, L103–L105. doi: 10.1086/182029

Meier, D. L. (1976b). The optical appearance of model primeval galaxies. *Astrophys. J.* 207, 343-350 doi: 10.1086/154500

Palanque-Delabrouille, N., Yeche, C. H., Myers, A. D., Petitjean, P., Ross, N. P., Sheldon, E., et al. (2011). Variability selected high-redshift quasars on SDSS Stripe 82. *Astron. Astrophys.* 530:A122. doi: 10.1051/0004-6361/201016254

Pâris, I., Petitjean, P., Ross, N. P., Myers, A. D., Aubourg, É., Streblyanska, A., et al. (2017). The sloan digital sky survey quasar catalog: twelfth data release. *Astrophys. J.* 597:A79. doi: 10.1051/0004-6361/201527999

Retana-Montenegro, E., and Röttgering, H. J. A. (2017). Probing the radio loud/quiet AGN dichotomy with quasar clustering *Astrophysics* 600:a197. doi: 10.1051/0004-6361/201526433

Richards, G. T., Fan, X., Newberg, H. J., Strauss, M. A., Vanden Berk, D. E., Schneider, D. P., et al. (2002). Spectroscopic target selection in the sloan digital sky survey: the quasar sample. *Astron. J.* 123:2945. doi: 10.1086/340187

Richards, G. T., Fan, X., Newberg, H. J., Strauss, M. A., Vande Berk, D. E., Schneider1, D. P., et al. (2006). Spectroscopic target selection in the sloan digital sky survey: the quasar sample. *Astron. J.* 131, 2766–2787. doi: 10.1086/503559

Ross, N. P., Myers, A. D., Sheldon, E. S., Yèche, C., Strauss, M. A., Bovy, J., et al. (2012). The SDSS-III baryon oscillation spectroscopic survey: quasar target selection for data release nine. *Astrophys. J.* 199:3. doi: 10.1088/0067-0049/199/1/3

Ross, N. P., Shen, Y., Strauss, M. A., Vanden Berk, D. E., Connolly, A. J., Richards, G. T., et al. (2009). Clustering of low-redshift (z <= 2.2) quasars from the sloan digital sky survey. *Astrophys. J.* 697:1634. doi: 10.1088/0004-637X/697/2/1634

Röttgering, H., Afonso, J., Barthel, P., Batejat, F., Best, P., Bonafede, A., et al. (2011). LOFAR and APERTIF surveys of the radio sky: probing shocks and magnetic fields in galaxy clusters. *J. Astrophys. Astron.* 32, 557–566. doi: 10.1007/s12036-011-9129-x

Salvato, M., Hasinger, G., Ilbert, O., Zamorani, G., Brusa, M., Scoville, N. Z., et al. (2009). Photometric redshift and classification for the XMM-COSMOS sources. *Astrophys. J.* 690, 1250–1263. doi: 10.1088/0004-637X/690/2/1250

Salvato, M., Ilbert, O., Hasinger, G., Rau, A., Civano, F., Zamorani, G., et al. (2011). Dissecting photometric redshift for active galactic nucleus using XMM- and chandra-COSMOS samples. *Astrophys. J.* 742:61. doi: 10.1088/0004-637X/742/2/61

Sandage, A., Véron, P., and Wyndham, J. D. (1965). Optical identification of new quasi-stellar radio sources. *Astrophys. J.* 142:1307. doi: 10.1086/148415

Schneider, D. P., Richards, G. T., Hall, P. B., Strauss, M. A., Anderson, S. F., Boroson, T. A., et al. (2010). The sloan digital sky survey quasar catalog. V. Seventh data release. *Astron. J.* 139:2360. doi: 10.1088/0004-6256/139/6/2360

Shimwell, T. W., Röttgering, H. J. A., Best, P. N., Williams, W. L., Dijkema, T. J., de Gasperin, F., et al. (2017). The LOFAR two-metre sky survey. I. Survey description and preliminary data release. *Astron. Astrophys.* 598:A104. doi: 10.1051/0004-6361/201629313

Smolčić, V., Novak, M., Bondi, M., Ciliegi, P., Mooley, K. P., Schinnerer, E., et al. (2017). The VLA-COSMOS 3 GHz large project: continuum data and source catalog release. *Astron. Astrophys.* 602:A1. doi: 10.1051/0004-6361/201628704

Tyson, J. A. (2002). Large synoptic survey telescope: overview. *Proc. SPIE* 4836, 10–20. doi: 10.1117/12.456772

van Haarlem, M. P., Wise, M. W., Gunst, A. W., Heald, G., McKean, J. P., Hessels, J. W. T., et al. (2013). LOFAR: the LOw-Frequency ARray. *Astron. Astrophys.* A2:556. doi: 10.1051/0004-6361/201220873

Williams, W., Intema, H. T., and Röttgering, H. J. A. (2013). T-RaMiSu: the two-meter radio mini survey. I. The Boötes field. *Astron. Astrophys.* 549:A55. doi: 10.1051/0004-6361/201220235

Williams, W., van Weeren, R. J., Röttgering, H. J. A., Best, P., Dijkema, T. J., de Gasperin, F., et al. (2016). LOFAR 150-MHz observations of the Boötes field: catalogue and source counts. *Month. Notices RAS* 460:2385. doi: 10.1093/mnras/stw1056

Willott, C. J., Philippe, P., Omont, A., Bergeron, J., Delfosse, X., Forveille, T., et al. (2007). Four quasars above redshift 6 discovered by the Canada-France high-z quasar survey. *Astrophys. J.* 134, 2435–2450. doi: 10.1086/522962

Wright, E. L., Eisenhardt, P. R. M., Mainzer, A. K., Ressler, M. E., Cutri, R. M., Jarrett, T., et al. (2010). The wide-field infrared survey explorer (WISE): mission description and initial on-orbit performance. *Astron. J.* 140, 1868–1881. doi: 10.1088/0004-6256/140/6/1868

York, D. G., Adelman, J., Anderson, J. E., Scott, F., Annis, J., Bahcall, N. A., et al. (2000). The sloan digital sky survey: technical summary. *Astron. J.* 120, 1579–1587. doi: 10.1086/301513

Yèche, N. P., Petitjean, P., Rich, J., Aubourg, E., Busca, N., Hamilton, J.-C., et al. (2010). Artificial neural networks for quasar selection and photometric redshift determination. *Astrophys. J.* 523:A14. doi: 10.1051/0004-6361/200913508

Zeimann, G. R., White, R. L., Becker, R. H., Hodge, J. A., Stanford, S. A., and Richards, G. T. (2011). Discovery of a radio-selected z ˜ 6 quasar. *Astrophys. J.* 746:57. doi: 10.1088/0004-637X/736/1/57

Conflict of Interest Statement: The authors declare that the research was conducted in the absence of any commercial or financial relationships that could be construed as a potential conflict of interest.

The reviewer, DB, and handling Editor declared their shared affiliation.